CHAPTER

Aerodynamic Modelling 12

12.1 Introduction

Probably the most difficult task confronting the flight dynamicist is the identification and quantification of the aerodynamic description of the aeroplane for use in the equations of motion. *Aerodynamic modelling* is concerned with the development of mathematical models to describe the aerodynamic forces and moments acting on the airframe. As the flow conditions around the airframe are generally complex, any attempt to describe the aerodynamic phenomena mathematically must result in compromise. Obviously, the most desirable objective is the most accurate mathematical description of the airframe aerodynamics as can possibly be devised. Unfortunately, even if accurate mathematical models can be devised, they are often difficult to handle in an analytical context and do not, in general, lend themselves to application to the linearised equations of motion.

The solution to the problem is to seek simpler approximate aerodynamic models which can be used in the equations of motion and which represent the aerodynamic properties of the airframe with acceptable accuracy. A consequence of this is that the aerodynamic models are only valid for a small range of operating conditions; therefore, the solution of the equations of motion is also valid only for the same limited range of conditions. By repeating this procedure at many points in the flight envelope of the aeroplane, an acceptable "picture" of its dynamic properties can be built up, subject of course to the limitations of the modelling techniques used.

In the present context, *aerodynamic stability and control derivatives* are used to model the aerodynamic properties of the aeroplane. The concept of the aerodynamic derivative as a means for describing aerodynamic force and moment characteristics is introduced and described in Chapter 4 (Section 4.2). The use of the aerodynamic derivative as a means for explaining the dependence of the more important dynamic characteristics of the aeroplane on its dominant aerodynamic properties is discussed in Chapters 6 and 7. In the illustrations, only those derivatives associated with the dominant aerodynamic effects are discussed. Clearly, if the most important aerodynamic properties ascribed to every derivative are known, a more subtle and expansive interpretation of aircraft dynamics may be made in the analysis of the response transfer functions. Thus, a good understanding of the origin, meaning, and limitation of the aerodynamic derivatives provides the means by which the flight dynamicist may achieve very considerable insight into the subtleties of aircraft dynamics and into flying and handling qualities. In the author's opinion, this knowledge is also essential for the designer of stability augmentation systems for the reasons illustrated in Chapter 11.

This chapter is concerned with a preliminary review of, and introduction to, aerodynamic stability and control derivatives at the simplest level consistent with the foregoing material.

However, it must be remembered that alternative methods for aerodynamic modelling are commonly in use when rather greater detail is required in the equations of motion. For example, in continuous simulation models, the equations of motion may well be non-linear and the aerodynamic models are correspondingly rather more complex. Today, it is common practice to investigate analytically the dynamic behaviour of combat aircraft at very high angles of incidence, conditions which may be grossly non-linear and for which the aerodynamic derivative would be incapable of providing an adequate description of the aerodynamics. For such applications experimental or semi-empirical sources of aerodynamic information are more appropriate.

Whatever the source of the aerodynamic models, simple or complex, the best that can be achieved is an *estimate* of the aerodynamic properties. This immediately prompts the question, *how good is the estimate*? This question is not easy to answer and depends ultimately on the confidence in the aerodynamic modelling process and the fidelity of the aircraft dynamics derived from the aerodynamic model.

12.2 Quasi-static derivatives

To appreciate the "meaning" of the aerodynamic derivative, consider, for example, the derivative which quantifies *normal force due to rate of pitch*, denoted

$$\overset{\circ}{Z}_q = \frac{\partial Z}{\partial q} \tag{12.1}$$

The component of normal force experienced by the aircraft resulting from a pitch velocity perturbation is therefore given by

$$Z = \overset{\circ}{Z}_q\, q \tag{12.2}$$

Now, in general, the disturbance giving rise to the pitch rate perturbation also includes perturbations in the other motion variables, which give rise to additional components of normal force as indicated by the appropriate terms in the aerodynamic normal force model in equations (4.37). However, when considering the derivative $\overset{\circ}{Z}_q$ it is usual to consider its effect in isolation, as if the perturbation comprised only pitch rate. Similarly, the effects of all the other derivatives are considered in isolation by assuming the perturbation to comprise only the motion appropriate to the derivative in question.

By definition, the equations of motion, equations (4.37), in which the derivatives appear describe small perturbation motion about a steady trimmed equilibrium flight condition. Thus, for example, in the undisturbed state the component of normal force Z given by equation (12.2) is zero since the perturbation variable q is zero. Similarly, all aerodynamic force and moment components in all small perturbation equations of motion are zero at the trim condition. The point of this perhaps obvious statement is to emphasise that, in the present context, the aerodynamic derivatives only play a part in determining the motion of the aeroplane when it is in a state of "dynamic upset" with respect to its initial trim condition. As described in earlier chapters, the state of dynamic upset is referred to equivalently as a perturbation about the equilibrium condition, and it is usually transient. Thus, to be strictly applicable to the dynamic conditions they describe, the derivatives should be expressed in terms of the non-steady aerodynamic conditions they attempt to quantify. Clearly a difficult demand!

Since the motion of interest is limited, by definition, to small perturbations about equilibrium then, in the limit, the perturbations tend to zero and the dynamic condition becomes coincident with the equilibrium flight condition. It is therefore common practice to evaluate the aerodynamic derivatives at the steady equilibrium condition and to assume that they are applicable to the small perturbation motion about that equilibrium. This procedure gives rise to the so-called *quasi-static aerodynamic derivatives*—quantities based on, and derived from, static aerodynamic conditions but used in the description of dynamically varying aerodynamic conditions. Aerodynamic derivatives obtained by this means seem to be quite adequate for studies of small perturbation dynamics but, not surprisingly, become increasingly inappropriate as the magnitude of the perturbation is increased. As suggested previously, studies of large amplitude dynamics require rather more sophisticated methods of aerodynamic modelling.

To illustrate the concept of the quasi-static derivative, consider the contribution of aerodynamic drag D to the axial force X acting on the aircraft in a disturbance. Assuming that the aircraft axes are wind axes, then

$$X = -D \tag{12.3}$$

A typical plot of aerodynamic drag against velocity is shown in Fig. 12.1. Let the steady equilibrium velocity be V_0 at the flight condition of interest which defines the operating point p on the plot. Now let the aeroplane be subjected to a disturbance giving rise to a small velocity perturbation $\pm u$ about the operating point as indicated. The derivative *axial force due to velocity* is defined as

$$\overset{\circ}{X}_u = \frac{\partial X}{\partial U} \equiv \frac{\partial X}{\partial V} \tag{12.4}$$

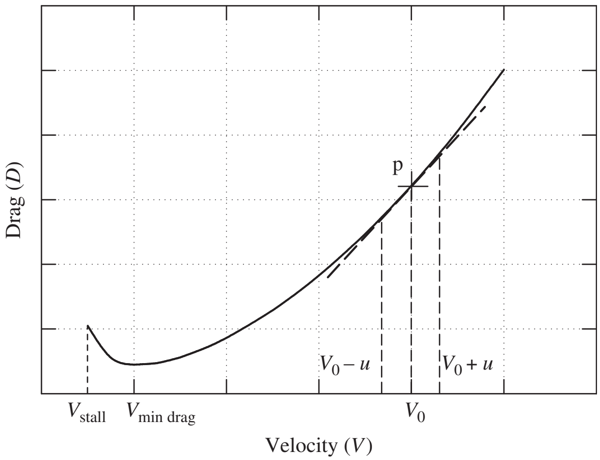

FIGURE 12.1 Typical aerodynamic drag-velocity characteristic.

where the total perturbation velocity component along the x axis is given by

$$U = U_e + u \equiv V_0 + u \equiv V \tag{12.5}$$

Whence

$$\mathring{X}_u = -\frac{\partial D}{\partial V} \tag{12.6}$$

and the slope of the drag-velocity plot at p gives the quasi-static value of the derivative $\mathring{X}_u$ at the flight condition corresponding with the trimmed velocity V_0. Some further simple analysis is possible since the drag is given by

$$D = \tfrac{1}{2}\rho V^2 S C_D \tag{12.7}$$

Assuming the air density ρ remains constant, since the perturbation is small, then

$$\frac{\partial D}{\partial V} = \tfrac{1}{2}\rho V S\left(2C_D + V\frac{\partial C_D}{\partial V}\right) \tag{12.8}$$

To define the derivative $\mathring{X}_u$ at the flight condition of interest, let the perturbation become vanishingly small such that $u \rightarrow 0$ and hence $V \rightarrow V_0$. Then, from equations (12.6) and (12.8),

$$\mathring{X}_u = -\tfrac{1}{2}\rho V_0 S\left(2C_D + V_0\frac{\partial C_D}{\partial V}\right) \tag{12.9}$$

where C_D and $\partial C_D/\partial V$ are evaluated at velocity V_0. Thus in order to evaluate the derivative the governing aerodynamic properties are *linearised about the operating point* of interest, which is a direct consequence of the assumption that the perturbation is small. A similar procedure enables all of the aerodynamic stability and control derivatives to be evaluated, although the governing aerodynamic properties may not always lend themselves to such simple interpretation.

It is important to note that in the previous illustration the derivative $\mathring{X}_u$ varies with velocity. In general, most derivatives vary with velocity, or Mach number, altitude, and incidence. In fact many derivatives demonstrate significant and sometimes abrupt changes over the flight envelope, especially in the transonic region.

12.3 Derivative estimation

A number of methods are used to evaluate the aerodynamic derivatives. However, whichever method is used, the resulting evaluations can, at best, be regarded only as *estimates* of the exact values. The degree of confidence associated with the derivative estimates is dependent on the quality of the aerodynamic source material and the method of evaluation used. It is generally possible to obtain estimates of the longitudinal aerodynamic derivatives with a greater degree of confidence than can usually be ascribed to estimates of the lateral-directional aerodynamic derivatives.

12.3.1 Calculation

The calculation of derivatives from first principles using approximate mathematical models of airframe aerodynamic properties is probably the simplest and least accurate method of estimation. In particular, it can provide estimates of questionable validity, especially for the lateral-directional derivatives. However, since the approximate aerodynamic models are based on an understanding of the physical phenomena involved, simple calculation confers significant advantage as a means for gaining insight into the dominant aerodynamic properties driving the airframe dynamics. Thus an appreciation of the theoretical methods for estimating aerodynamic derivatives provides a sound foundation on which to build most analytical flight dynamics studies.

To improve on the often poor derivative estimates obtained by calculation, *semi-empirical* methods of estimation have evolved in the light of experience gained from the earliest days of aviation to the present day. Semi-empirical methods are based on simple theoretical calculation modified with the addition of generalised aerodynamic data obtained from experimental sources and accumulated over many years. They are generally made available in various reference documents, and today many are also available as interactive computer programs. In the United Kingdom the Engineering Sciences Data Unit (ESDU) publishes a number of volumes on aerodynamics, some of which are specifically concerned with aerodynamic derivative estimation. Similar source material is also published in the United States (by DATCOM) and elsewhere.

Use of semi-empirical data items requires, at the outset, some limited information about the geometry and aerodynamics of the subject aeroplane. The investigator then works through the estimation process, which involves calculation and frequent reference to graphical data and nomograms, to arrive at an estimate of the value of the derivative at the flight condition of interest. Such is the state of development of these methods that it is now possible to obtain derivative estimates of good accuracy, at least for aeroplanes having conventional configurations.

Because of the recurring need to estimate aircraft stability and control derivatives, a number of authors have written computer programs to calculate derivatives with varying degrees of success. Indeed, a number of the ESDU data items are now available as computer software. The program by Mitchell (1973) and its subsequent modification by Ross and Benger (1975) has enjoyed some popularity, especially for preliminary estimates of the stability and control characteristics of new aircraft configurations. The text by Smetana (1984) also includes listings for a number of useful computer programs concerned with aircraft performance and stability.

12.3.2 Wind tunnel measurement

The classical wind tunnel test is one in which a reduced scale model of the aircraft is attached to a balance and the six components of force and moment are measured for various combinations of wind velocity, incidence angle, sideslip angle, and control surface angle. The essential feature of such tests is that the conditions are *static* when the measurements are made. Provided they are carefully designed and executed, wind tunnel tests can give good estimates of the force-velocity and moment-velocity derivatives in particular. Scale effects can give rise to accuracy problems, especially when difficult full scale flight conditions are simulated; although some derivatives can be estimated with good accuracy, it may be very difficult to devise experiments to adequately measure others. However, despite the limitations of the experimental methods, measurements are made for real aerodynamic flow conditions, and in principle it is possible to obtain derivative estimates of greater fidelity than is likely by calculation.

Dynamic, or non-stationary, experiments can be conducted, from which estimates for the force-rotary and moment-rotary derivatives can be made. The simplest of these requires a special rig in which to mount the model which enables the model to undergo a single degree of freedom free or forced oscillation in roll, or in pitch, or in yaw. Analysis of the oscillatory time response obtained in such an experiment enables estimates to be made of the relevant damping and stiffness derivatives. For example, an oscillatory pitch experiment enables estimates to be made of $\mathring{M}_q$ and $\mathring{M}_w$. More complex multi-degree of freedom test rigs become necessary when the intent is to measure the motion coupling derivatives—for example, yawing moment due to roll rate $\mathring{N}_p$. As the experimental complexity is increased so the complexity of the analysis required to calculate the derivative estimates from the measurements is also increased and, consequently, it becomes more difficult to guarantee the accuracy of the derivatives thus obtained.

12.3.3 Flight test measurement

The estimation of aerodynamic derivatives from flight test measurements is an established and well developed experimental process. However, derivative estimates are usually obtained indirectly since it is not possible to measure the aerodynamic components of force and moment acting on the airframe directly. Also, since the aircraft has six degrees of freedom, it is not always possible to perturb the single motion variable of interest without perturbing some, or all, of the others as well. However, as in wind tunnel testing, some derivatives are easily estimated from flight test experiments with a good degree of confidence, whereas others can be notoriously difficult to estimate.

Although it is relatively easy to set up approximately steady conditions in flight from which direct estimates of some derivatives can be made—for example, a steady sideslip for the estimation of $\mathring{Y}_v$, $\mathring{L}_v$ and $\mathring{N}_v$—the technique often produces results of indifferent accuracy and has limited usefulness. Today *parameter identification* techniques are commonly used in which measurements are made following the deliberate excitation of multi-variable dynamic conditions. Complex multi-variable response analysis then follows, from which it is possible to derive a complete estimate of the mathematical model of the aircraft corresponding with the flight condition at which the measurements were made. Parameter identification is an analytical process in which full use is made of state-space computational tools to estimate the aircraft state description that best matches the input-output response measured in flight. It is essentially a multi-variable curve fitting procedure, and the computational output consists of the coefficients in the aircraft state equation from which estimates of the aerodynamic stability and control derivatives may be obtained. This method is complex, and success depends, to a considerable extent, on the correct choice of computational algorithm appropriate to the experiment.

A simple diagram containing the essential functions of the parameter identification procedure is shown in Fig. 12.2. A flight test exercise is undertaken in the fully instrumented subject aircraft, and the pilot applies control inputs designed to excite the dynamic response of interest. The control inputs and the full complement of dynamic response variables are recorded in situ or may be telemetered directly to a ground station for online analysis. The parameter identification process is entirely computational and is based on a mathematical model of the aeroplane which is deliberately

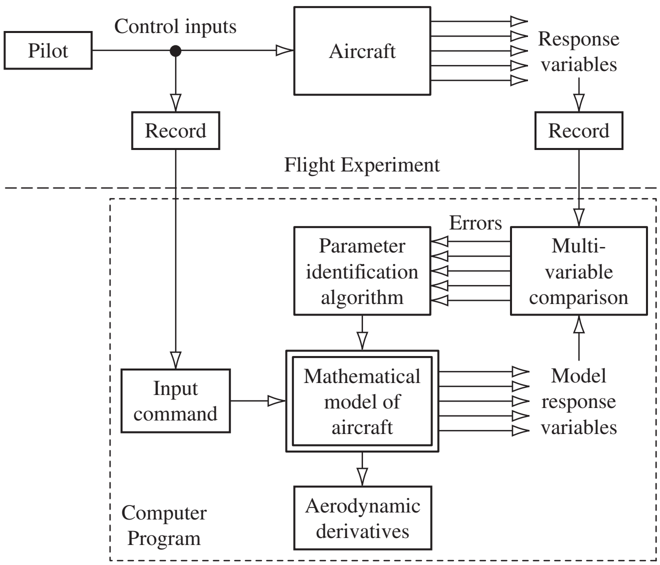

FIGURE 12.2 Parameter identification.

structured to include the terms appropriate to the flight experiment. The object is then to identify the coefficients in the aircraft model which give the best match with the dynamics of the experimental response. The recorded control inputs are applied to the model of the aircraft, and its multi-variable response is compared with the recorded response made in the flight experiment. Response matching errors are then used to adjust the coefficients in the aircraft model according to the parameter identification algorithm, and the process is repeated iteratively until the response matching errors are minimised.

All of the recorded signals contain noise, measurement errors, and uncertainties of various kinds to a greater or lesser extent. The complexity of the identification process is therefore magnified considerably since statistical analysis methods play an essential part in all modern algorithms. For example, Kalman filtering techniques are frequently used to first obtain consistent, and essentially error free, estimates of the state variables for subsequent use in the identification process. Typical commonly encountered parameter identification algorithms include the *equation error* method, the *maximum likelihood* method, and various methods based on *statistical regression*. The development of parameter identification methods for application to aeronautical problems has been the subject of considerable research over the last 25 years or so, and a vast wealth of published material is available. A more detailed discussion of the subject is well beyond the scope of this book.

Until recently few books have been published which are concerned with aircraft parameter identification, see Klein and Morelli (2006), for example. Most of the available material appears to be contained in research papers, but the interested reader will find a useful collection of aircraft related papers in AGARD (1979). It is rare to find published listings of parameter identification computer programs; thus the work by Ross and Foster (1976) is especially useful, if somewhat dated. Probably two of the more useful sources of information on current developments in aircraft parameter identification are the proceedings of the AIAA annual Flight Mechanics and biannual Flight Test conferences.

The main disadvantages of parameter identification methods include the requirement for substantial computational "power" and the essential need for recorded flight data of the very highest quality. Despite these constraints, the process is now used routinely by many leading flight test organisations. Given adequate resources, the advantages of parameter identification are significant. All of the aerodynamic stability and control derivatives can be estimated in one pass, and the dynamic conditions to which they relate do not necessarily have to be linear. For example, it is now routinely possible to identify aircraft models in extreme manoeuvring conditions such as stall, spin, and at very high angles of attack when the aerodynamics are substantially non-linear. It is interesting that this method can also be used for estimating aerodynamic derivatives from "dynamic" wind tunnel experiments.

12.4 The effects of compressibility

The onset of compressible flow conditions gives rise to changes in the aerodynamic properties of the aeroplane which in general lead to corresponding changes in the stability and control characteristics. Clearly, this means a change in the flying and handling qualities of the aeroplane as the Mach number envelope is traversed. Typically, compressibility effects begin to become apparent at a Mach number of approximately 0.3, although changes in the stability and control characteristics may not become significant until the Mach number reaches 0.6 or higher. As Mach number increases the changes due to compressibility are continuous and gradual. However, in the transonic flow regime changes can be dramatic and abrupt. When appropriate, it is therefore important that the aerodynamic changes arising from the effects of compressibility are allowed for in even the simplest and most approximate aerodynamic derivative estimation.

An interesting chapter on the effects of compressibility on aircraft stability, control, and handling may be found in Hilton (1952). However, it must be remembered that, although at the time the book was written the problems were very clearly recognised, the mathematical models used to describe the phenomena were in most cases at an early stage of development. Today, sophisticated computational tools are commonly used to deal with the problems of modelling compressible aerodynamics. Nevertheless, the simpler models described by Hilton (1952) are still applicable, as is shown in the following sections, provided their limitations are appreciated.

12.4.1 Some useful definitions

Mach number M is defined as the ratio of the local flow velocity V to the local speed of sound a. Whence

$$\mathrm{M} = \frac{V}{a} \tag{12.10}$$

The *critical Mach number* M_{crit} is the free stream Mach number at which the local flow Mach number just reaches unity at some point on the airframe. In general, $\mathrm{M}_{crit} \leq 1.0$ and is typically in the order of 0.9.

Subsonic flight commonly refers to local aerodynamic flow conditions where $M < 1.0$. Practically, this means that the free stream Mach number is less than approximately 0.8. *Transonic flight* usually refers to generally subsonic flight but where the local flow Mach number $M \geq 1.0$. Transonic flight conditions are assumed when the free stream Mach number lies in the range $0.8 < M_0 < 1.2$. The greatest degree of aerodynamic unpredictability is associated with this Mach number range. *Supersonic flight* commonly refers to aerodynamic flow conditions when $M > 1.0$ everywhere in the local flow field. As with transonic conditions, supersonic flow conditions are assumed when the free stream Mach number is greater than approximately 1.2.

A *shock wave* is a compression wave front which occurs in the supersonic flow field around an airframe. A shock wave originating at a point on the airframe, such as the nose, is initially a plane wave front normal to the direction of the flow. As the flow Mach number is increased, the shock wave becomes a conical wave front, or *Mach cone*, the apex angle of which decreases with increasing Mach number. As the air flow traverses the shock wave, it experiences an abrupt increase in pressure, density, and temperature, and the energy associated with these changes is extracted from the total flow energy to result in reduced velocity behind the wave front. Collectively, these changes are seen as an abrupt increase in drag in particular and may be accompanied by significant changes in trim and in the stability and control characteristics of the aeroplane.

The *shock stall* is sometimes used to describe the abrupt aerodynamic changes experienced when an aeroplane accelerating through the transonic flight regime first reaches the critical Mach number. At the critical Mach number, shock waves begin to form at various places on the airframe and are accompanied by abrupt reduction in local lift, abrupt increase in local drag, and some associated change in pitching moment. Since the effect of these aerodynamic changes is not unlike that of the classical low speed stall, it is referred to as the shock stall. However, unlike the classical low speed stall, the aeroplane continues to fly through the condition.

12.4.2 Aerodynamic models

Because of the aerodynamic complexity of the conditions applying to an aeroplane in a compressible flow field, it is difficult to derive other than the very simplest mathematical models to describe those conditions. Thus for analytical application, as required in aerodynamic derivative estimation, mathematical modelling is usually limited to an approximate description of the effects of compressibility on the lifting surfaces of the aeroplane only. In particular, the ease with which the aerodynamic properties of a wing in compressible flow can be estimated is dependent, to a large extent, on the leading edge flow conditions.

As flow Mach number is increased to unity, a shock wave forms a small distance ahead of the leading edge of a typical wing and the shock wave is said to be *detached*. As the Mach number is increased further, the shock wave moves nearer to the leading edge of the wing and eventually moves onto the wing when it is said to be *attached*. Since the flow velocity behind the shock wave is lower than the free stream value, when the shock wave is detached the leading edge of the wing is typically in subsonic flow. In this condition the pressure distribution on the wing, in particular, the leading edge suction peak, is subsonic and the aerodynamic characteristics of the wing are quite straightforward to estimate. However, when the shock wave is attached, the leading edge of the wing is typically in supersonic flow and estimation of the aerodynamic properties, in particular, the drag rise, is much less straightforward. Since the incident flow velocity direction is always considered perpendicular to the leading edge of the wing, it is always lower on a swept wing because it is equivalent to the free stream velocity resolved through the leading edge sweep angle. Further, since wing sweep brings more, or more likely, all of the wing within the Mach cone, the high drag associated with a supersonic leading edge is reduced or avoided altogether for a larger range of supersonic Mach numbers.

12.4.3 Subsonic lift, drag, and pitching moment

The theoretical maximum value of lift curve slope for a rectangular flat plate wing of infinite span in incompressible flow is given by

$$a_\infty = 2\pi\cos\Lambda_{le} \quad \text{rad}^{-1} \tag{12.11}$$

where Λ_{le} is the leading edge sweep angle. For a wing of finite thickness this value of lift curve slope is reduced, and Houghton and Carpenter (1993) give an approximate empirical expression which is a function of geometric thickness to chord ratio *t/c* such that equation (12.11) becomes

$$a_\infty = 1.8\pi\left(1 + 0.8\frac{t}{c}\right)\cos\Lambda_{le} \quad \text{rad}^{-1} \tag{12.12}$$

For a wing of finite span the lift curve slope is reduced further as a function of aspect ratio A and is given by the expression

$$a = \frac{a_\infty}{\left(1 + \dfrac{a_\infty}{\pi A}\right)} \tag{12.13}$$

For Mach numbers below M_{crit}, but when the effects of compressibility are evident, the *Prandtl-Glauert rule* provides a means for estimating the lifting properties of a wing. For an infinite span wing with leading edge sweep angle Λ_{le}, the lift curve slope a_{∞_c} in the presence of compressibility effects is given by

$$a_{\infty_c} = \frac{a_{\infty_i}}{\sqrt{1 - M^2\cos^2\Lambda_{le}}} \tag{12.14}$$

where, a_{∞_i} is the corresponding incompressible lift curve slope given, for example, by equation (12.12). An equivalent expression for a wing of finite span with aspect ratio A is quoted in Babister (1961) and is given by

$$a_c = \frac{(A + 2\cos\Lambda_{le})a_{\infty_i}}{2\cos\Lambda_{le} + A\sqrt{1 - M^2\cos^2\Lambda_{le}}} \tag{12.15}$$

For Mach numbers below M_{crit}, the zero lift drag coefficient C_{D_0} remains at its nominal incompressible value and the changes in drag due to the effects of compressibility result mainly from the induced drag contribution. Thus the classical expression for the drag coefficient applies:

$$C_{D_c} = C_{D_0} + kC_{L_c}^2 = C_{D_0} + ka_c^2\alpha^2 \tag{12.16}$$

In general, the effect of compressibility on pitching moment coefficient in subsonic flight is small and is often disregarded. However, in common with lift and drag coefficient, such changes in pitching moment coefficient as may be evident increase as the Mach number approaches unity. Further, these changes are more pronounced in aircraft with a large wing sweep angle and result from a progressive aft shift in aerodynamic centre. Since the effect is dependent on the inverse of $\sqrt{1-M^2\cos^2\Lambda_{le}}$, or its equivalent for a wing of finite span, it does not become significant until, approximately, $M \geq 0.6$.

It is important to appreciate that the Prandtl-Glauert rule applies to subsonic flight only in the presence of the effects of compressibility. The models given previously become increasingly inaccurate at Mach numbers approaching and exceeding unity. In other words, the Prandtl-Glauert rule is not applicable to transonic flight conditions.

12.4.4 Supersonic lift, drag, and pitching moment

The derivation of simple approximate aerodynamic models to describe lift, drag, and pitching moment characteristics in supersonic flow conditions is much more difficult. Such models as are available depend on the location of the shocks on the principal lifting surfaces and, in particular, on whether the leading edge of the wing is subsonic or supersonic. In every case the aerodynamic models require a reasonable knowledge of the geometry of the wing, including the aerofoil section. The three commonly used theoretical tools are, in order of increasing complexity, the linearised *Ackeret theory*, the second order *Busemann theory*, and the *shock expansion* method. A full discussion of these is not appropriate here, and only the simplest linear models are summarised. The material is included in most aerodynamics texts, such as Bertin and Smith (1989) and Houghton and Carpenter (1993).

The lift curve slope of an infinite span swept wing in supersonic flow, which implies a supersonic leading edge condition, is given by

$$a_{\infty_c} = \frac{4\cos\Lambda_{le}}{\sqrt{M^2\cos^2\Lambda_{le}-1}} \tag{12.17}$$

Clearly, equation (12.17) is valid only for Mach number $M > \sec\Lambda_{le}$; at lower Mach number the leading edge is subsonic since it is within the Mach cone. For a wing of finite span the expression given by equation (12.17) is "corrected" for aspect ratio. Thus

$$a_c = a_{\infty_c}\left(1 - \frac{1}{2A\sqrt{M^2\cos^2\Lambda_{le}-1}}\right) \tag{12.18}$$

and the parameter $A\sqrt{M^2\cos^2\Lambda_{le}-1}$ is termed the *effective aspect ratio* by Liepmann and Roshko (1957).

The drag of an aeroplane in supersonic flight is probably one of the most difficult aerodynamic parameters to estimate with any accuracy. The drag of a wing with a supersonic leading edge comprises three components: the *drag due to lift*, the *wave drag*, and the *skin friction drag*. The drag due to lift, sometimes known as *wave drag due to lift*, is equivalent to the induced drag in subsonic flight. Wave drag, also known as *form drag* or *pressure drag*, occurs only in compressible flow conditions and is a function of aerofoil section geometry. Skin friction drag is the same as the familiar zero lift drag in subsonic flight, which is a function of wetted surface area.

A simple approximate expression for the drag coefficient of an infinite span swept wing in supersonic flight is given by

$$C_{D_\infty} = \frac{4\alpha^2 \cos\Lambda_{le}}{\sqrt{M^2\cos^2\Lambda_{le} - 1}} + \frac{k\left(\frac{t}{c}\right)^2 \cos^3\Lambda_{le}}{\sqrt{M^2\cos^2\Lambda_{le} - 1}} + C_{D_0} \tag{12.19}$$

where the first term is the drag coefficient due to lift, the second term is the wave drag coefficient, and the third term is the zero lift drag coefficient. Here, in the interest of simplicity, the wave drag is shown to be dependent only on the ratio of aerofoil section thickness to chord ratio, *t*/*c*, which implies that the section is symmetrical. When the section has camber, the wave drag includes a second term which is dependent on the square of the local angle of attack with respect to the mean camber line. The camber term is not included in equation (12.19) because many practical supersonic aerofoils are symmetric or near symmetric. The constant k is also a function of the aerofoil section geometry and is 2/3 for bi-convex or typical modified double wedge sections, both of which are symmetric.

For a finite span wing with aspect ratio A the drag coefficient is given very approximately by

$$C_{D_\infty} = \left(\frac{4\alpha^2 \cos\Lambda_{le}}{\sqrt{M^2\cos^2\Lambda_{le} - 1}} + \frac{k\left(\frac{t}{c}\right)^2 \cos^3\Lambda_{le}}{\sqrt{M^2\cos^2\Lambda_{le} - 1}}\right)\left(1 - \frac{1}{2A\sqrt{M^2\cos^2\Lambda_{le} - 1}}\right) + C_{D_0} \tag{12.20}$$

It is assumed that the wing to which equation (12.20) relates is of constant thickness with span and that it has a rectangular planform, which is most unlikely for a real, practical wing. Alternative and rather more complex expressions can be derived which are specifically dependent on wing geometry to a much greater extent. However, there is no guarantee that the estimated drag coefficient is more accurate since it remains necessary to make significant assumptions about the aerodynamic operating conditions of the wing.

It is also difficult to obtain a simple and meaningful expression for pitching moment coefficient in supersonic flight conditions. However, it is relatively straightforward to show that, for an infinite span flat plate wing, the aerodynamic centre moves aft to the half chord point in supersonic flow. This results in an increase in nose down pitching moment together with an increase in the longitudinal static stability margins, with corresponding changes in the longitudinal trim, stability, and control characteristics of the aeroplane. An increase in thickness and a reduction in aspect ratio of the wing causes the aerodynamic centre to move forward from the half chord point with a corresponding reduction in stability margins. Theoretical prediction of these changes for anything other than a simple rectangular wing is not generally practical.

12.4.5 Summary

It is most important to realise that the aerodynamic models outlined in Sections 12.4.3 and 12.4.4 describe, approximately, the properties of the main lifting wing of the aeroplane only. Since the wing provides most of the lift, with perhaps smaller contributions from the fuselage and tailplane, or foreplane, it is expected that equations (12.15) and (12.18) would give a reasonable indication of the lift curve slope of a complete aeroplane. However, this is not necessarily expected of the drag estimates given by equations (12.16) and (12.20). The drag contributions from the fuselage and tailplane, or foreplane, may well be a large fraction of the total, so estimates obtained with these equations should be treated accordingly. It is suggested that the main purpose of the material given in Sections 12.4.3 and 12.4.4 is to provide an appreciation of the primary aerodynamic effects of compressibility as they relate to stability and control and to provide a means for checking estimates obtained by other, especially computational, means.

Little mention has been made of the transonic flight regime, for the simple reason that analytical models suitable for the estimation of aerodynamic stability and control properties at the present level of interest are not available. Considerable research has been undertaken in recent years into transonic aerodynamics, but the analysis remains complex and has found greatest use in computational methods for flow prediction. When it is necessary to have estimates of the aerodynamic properties of a complete aeroplane configuration in compressible flow conditions, reference to source material such as the ESDU data items is preferable.

Today, increasing use is made of computational methods for estimating the aerodynamic properties of complete aeroplane configurations, at all flight conditions. Provided the geometry of the airframe can be described in sufficient detail, computational methods, such as the *vortex lattice method* or the *panel method*, can be used to obtain estimates of aerodynamic characteristics at acceptable levels of accuracy. By such means, aerodynamic information can be obtained for conditions which would otherwise be impossible using analytical methods.

EXAMPLE 12.1

A substantial database of aerodynamic stability and control parameters for the McDonnell-Douglas F-4C Phantom aircraft is provided by Heffley and Jewell (1972). Data are given for altitudes from sea level to 55,000 ft and for Mach numbers from 0.2 to 2.2, and the aircraft shows most of the classical effects of translation from subsonic to supersonic flight. Some limited additional information was obtained from Jane's (1969–1970). The main geometric parameters of the aircraft used in the example are

Wing area (reference area)	$S = 530\ \text{ft}^2$
Wing span	$b = 38.67\ \text{ft}$
Mean geometric chord (reference chord)	$\bar{c} = 16.04\ \text{ft}$
Average thickness–chord ratio	$t/c = 0.051$
Aspect ratio	$A = 2.82$
Leading edge sweep angle	$\Lambda_{le} = 50\ \text{deg}$
Centre of gravity position	$h = 0.289$

The lift, drag, and pitching moment characteristics are summarised in Fig. 12.3 as a function of Mach number for two altitudes, 15,000 ft and 35,000 ft, because the data for these two altitudes extend over the entire Mach number envelope.

Lifting properties are represented by the plot of lift curve slope a as a function of Mach number. The effect of compressibility becomes obvious at Mach 0.8 at the onset of the transonic flow regime. The lift curve slope reaches a maximum at Mach 1.0, and its gentle reduction

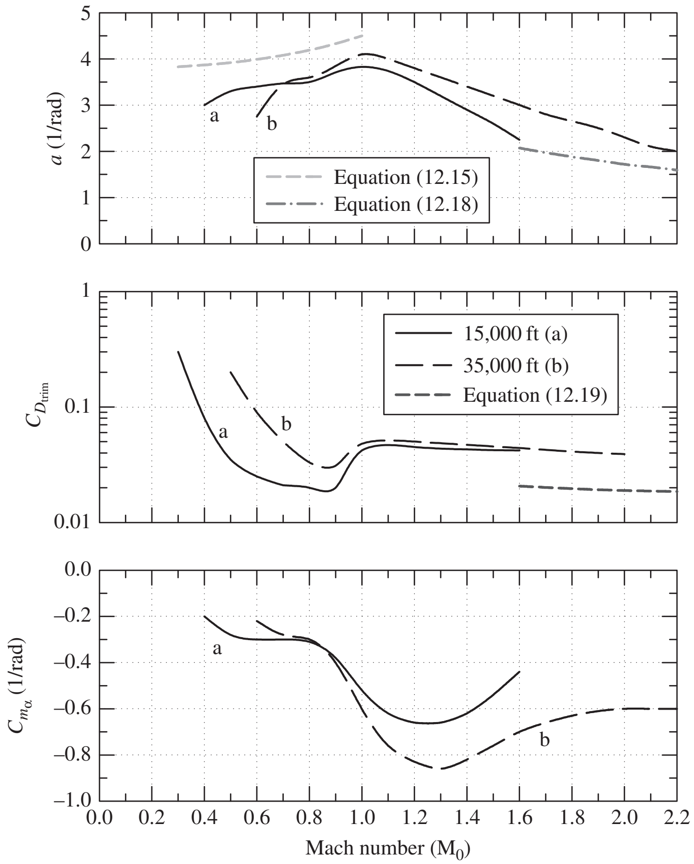

FIGURE 12.3 Lift, drag, and pitching moment variation with Mach number.

thereafter is almost linear with Mach number. The Prandtl-Glauert rule approximation, as given by equation (12.15), is shown for comparison in the subsonic Mach number range. The approximation assumes a 2D lift curve slope calculated according to equation (12.12) and shows the correct trend; however, it gives an overestimate of total lift curve slope. The linear supersonic approximation for lift curve slope, as given by equation (12.18), is also shown for completeness. In this case the 2D lift curve slope was calculated using equation (12.17). Again, the trend matches reasonably well, but the model gives a significant underestimate. It is prudent to recall at this juncture that both models describe the lift curve slope of a finite wing only, whereas the F-4C data describe the entire airframe characteristic.

The drag properties are represented by the trim drag coefficient, plotted on a logarithmic scale, as a function of Mach number. The use of a logarithmic scale helps to emphasise the abrupt drag rise at Mach 1.0. In the subsonic Mach number range, the drag coefficient reduces with increasing Mach number, the classical characteristic, which implies that the drag coefficient is dominated by the induced drag contribution, as might be expected. However, in supersonic flight the drag coefficient remains almost constant, the contribution due to lift is small as both C_L and α are small, and the main contributions are due to wave drag and skin friction.

Shown on the same plot is the supersonic drag coefficient calculated according to equation (12.19) and clearly the match is poor. The trend is correct, but the magnitude is about half the actual airframe value. Once again, it should be remembered that equation (12.19) relates to a finite wing and not to a complete airframe. It is reasonably easy to appreciate that the fuselage and tail surfaces make a significant contribution to the overall drag of the aeroplane. Careful scrutiny of the aerodynamic data for 35,000 ft enables the expression for the subsonic drag coefficient, equation (12.16), to be estimated as

$$C_D = C_{D_0} + kC_L^2 = 0.017 + 0.216C_L^2 \tag{12.21}$$

This expression gave a good fit to the actual data, and the value of C_{D_0} was used in the evaluation of the supersonic drag coefficient, equation (12.19).

The final plot in Fig. 12.3 represents the effect of Mach number on pitching moment and shows the variation in the slope, denoted C_{m_α}, of the C_m-α curve as a function of Mach number. Since C_{m_α} is proportional to the controls-fixed static margin, it becomes more negative as the aerodynamic centre moves aft. This is clearly seen in the plot, and the increase in stability margin commences at a Mach number of 0.8. Now the relationship between controls-fixed stability margin, neutral point, and centre of gravity locations is given by equation (3.17):

$$K_n = h_n - h \tag{12.22}$$

With reference to Appendix 8, the expression for the derivative M_w is given by

$$M_w = \frac{\partial C_m}{\partial \alpha} = -aK_n \tag{12.23}$$

Thus, from equations (12.22) and (12.23), an expression for the location of the controls-fixed neutral point is easily calculated:

$$h_n = h - \frac{1}{a}\frac{\partial C_m}{\partial \alpha} \equiv h - \frac{1}{a}C_{m_\alpha} \tag{12.24}$$

Using equation (12.24) with the F-4C data for an altitude of 15,000 ft, the variation in neutral point position as a function of Mach number was calculated and the result is shown in Fig. 12.4.

Since the neutral point corresponds with the centre of pressure for the whole aeroplane, its aft shift with Mach number agrees well with the predictions given by "simple" aerofoil theory. Over the transonic Mach number range, the neutral point moves back to the midpoint of the mean aerodynamic chord and then moves forward a little at higher Mach numbers. It is interesting that at subsonic Mach numbers the neutral point remains more or less stationary at around $0.37\bar{\bar{c}}$, which is quite typical for many aeroplanes.

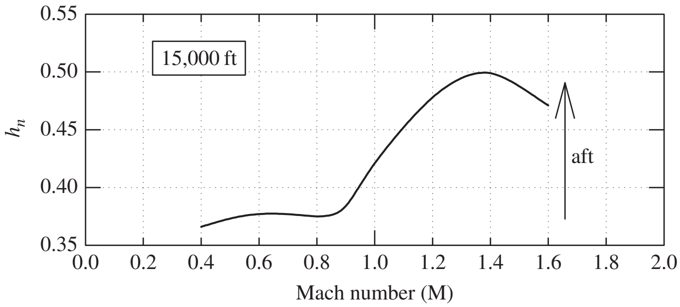

FIGURE 12.4 Variation of controls-fixed neutral point position with Mach number.

12.5 Limitations of aerodynamic modelling

Simple expressions for the aerodynamic stability and control derivatives may be developed from first principles based on analysis of the aerodynamic conditions following an upset from equilibrium. The cause of the upset may be external, the result of a gust for example, or internal, the result of a pilot control action. It is important to appreciate that in either event the disturbance is of short duration and that the controls remain fixed at their initial settings for the duration of the response. As explained in Section 12.2, the derivatives are then evaluated by linearising the aerodynamics about the nominal operating, or trim, condition. The aerodynamic models thus derived are limited in their application to small perturbation motion about the trim condition only. The simplest possible analytical models for the aerodynamic stability and control derivatives are developed, subject to the limitations outlined in this chapter, and described in Chapter 13.

References

AGARD. (1979). *Parameter Identification*. Lecture Series, AGARD-LS-104. Advisory Group for Aerospace Research & Development, 7 Rue Ancelle 92200, Neuilly-sur-Seine, France.

Babister, A. W. (1961). *Aircraft Stability and Control*. Oxford: Pergamon Press.

Bertin, J. J., & Smith, M. L. (1989). *Aerodynamics for Engineers*. (Second Edition). New Jersey: Prentice Hall, Englewood Cliffs.

ESDU Aerodynamics Series (2006). Engineering Sciences Data, ESDU International Ltd., 27 Corsham Street, London. www.esdu.com.

Heffley, R. K., & Jewell, W. F. (1972). *Aircraft Handling Qualities Data*. Washington, D.C. 20546: National Aeronautics and Space Administration, NASA Contractor Report, NASA CR-2144.

Hilton, W. F. (1952). *High Speed Aerodynamics*. London: Longmans, Green and Co.

Houghton, E. L., & Carpenter, P. W. (1993). *Aerodynamics for Engineering Students*. (Fourth Edition). London: Edward Arnold.

Liepmann, H. W., & Roshko, A. (1957). *Elements of Gas Dynamics*. NewYork: John Wiley and Sons, Inc.

McDonnell-Douglas Corp. (1960). *USAF stability and control handbook (DATCOM)*. St Louis, MO: McDonnell-Douglas Corp.

Mitchell, C. G. B. (1973). *A Computer Programme to Predict the Stability and Control Characteristics of Subsonic Aircraft*. Royal Aircraft Establishment Technical Report, RAE TR-73079. Farnborough: Royal Aircraft Establishment.

Ross, A. J., & Benger, N. J. (1975). *Modifications to a Computer Program for Predicting the Stability and Control Characteristics of Subsonic Aircraft (RAE Technical Report TR-73079)*. Royal Aircraft Establishment Technical Memorandum, RAE Tech Memo FS 40. Farnborough: Royal Aircraft Establishment.

Ross, A. J., & Foster, G. W. (1976). *FORTRAN Programs for the Determination of Aerodynamic Derivatives from Transient Longitudinal or Lateral Responses of Aircraft*. Aeronautical Research Council, Current Papers, ARC-P 1344. London: Her Majesty's Stationery Office.

Smetana, F. O. (1984). *Computer Assisted Analysis of Aircraft Performance Stability and Control*. New York: McGraw Hill Book Co.

Taylor, J. W. R. (Ed.), (1969−70). *Jane's All The World's Aircraft*. London: Jane's Yearbooks, Haymarket Publishing.